

IN THE PURSUIT OF $X(5568)$ AND ITS CHARMED PARTNERJ.Y. Süngü¹, A. Türkan², E. Veli Veliev¹¹ Department of Physics, Kocaeli University, 41380 Izmit, Turkey² Özyeğin University, Department of Natural and Mathematical Sciences, Çekmeköy, Istanbul, Turkey

The recent observation by the DØ collaboration of the first tetraquark candidate with four different quark flavors (u, d, s and b) in the $B_s^0 \pi^\pm$ channel having a narrow structure, has still not been confirmed by other collaborations. Further independent experiments are required either to confirm the $X(5568)$ state or to set limits on its production. Though quantum numbers are not exactly clear, the results existing in the literature indicate that it is probably an axial-vector or scalar state candidate. In this study, mass and pole residue of the $X(5568)$ resonance assuming as a tightly bound diquark, with spin-parity both $J^P = 1^+$ or $J^{PC} = 0^{++}$ are calculated using two-point Thermal SVZ sum rules technique by including condensates up to dimension six. Moreover, its partner in the charm sector is also discussed. Investigations defining the thermal properties of $X(5568)$ and its charmed partner may provide valuable hints and information for the upcoming experiments such as CMS, LHCb and PANDA.

PACS numbers: 11.55.Hx;12.38.Mh;14.80.-j

1. Introduction

A new era began in the hadron spectroscopy in 2003 when Belle Collaboration announced the pioneering discovery of the enigmatic resonance $X(3872)$ [1]. Since then there has been an explosion in the discovery of exotic structures that cannot be placed into the well-tested quark model of hadrons. This group of particles are called XYZ states, to indicate their nature is unclear, emerged from the Belle, BaBar, BESIII, LHCb, CDF, DØ and other collaborations (for a review of these particles, see Refs. [2, 3, 4, 5]). The idea of the multiquark states was firstly put forward by Jaffe in 1977 [6]. Especially after the observation of $X(3872)$, this topic become very active research field in hadron physics.

After thirteen years from this discovery, a unique structure $X(5568)$ containing four different quark flavors such as $[bd][\bar{s}\bar{u}]$, $[bu][\bar{s}\bar{d}]$, $[su][\bar{b}\bar{d}]$ or $[sd][\bar{b}\bar{u}]$ was reported by the DØ Collaboration in the decays $X(5568) \rightarrow B_s^0 \pi^\pm$, $B_s^0 \rightarrow J/\psi \phi$, $J/\psi \rightarrow \mu^+ \mu^-$, $\phi \rightarrow K^+ K^-$. The exclusive features of the $X(5568)$ at the vicinity of $D\bar{D}^*$ threshold, the tiny width and the large isospin violation in production and decay, has opened up a new window in hadron spectroscopy. Possible quantum numbers for this state are

¹ Email: jyilmazkaya@kocaeli.edu.tr

$J^P = 0^+$, if the $B_s^0\pi^\pm$ is produced in an S-wave or $J^P = 1^+$, if the decay proceeds via the chain $X(5568) \rightarrow B_s^{*0}\pi^\pm, B_s^{*0} \rightarrow B_s^0\gamma$ and the photon is not reconstructed. The measured mass and width are $M_X = (5567.8 \pm 2.9(\text{stat})_{-1.9}^{+0.9}(\text{syst}))$ MeV, $\Gamma_X = (21.9 \pm 6.4(\text{stat})_{2.5}^{+5.0}(\text{syst}))$ MeV [7], respectively.

However the CDF and ATLAS Collaborations reported independently negative search results for the $X(5568)$ state [8, 9], while the DØ Collaboration collected additional evidence by adding B_s^0 mesons reconstructed in semileptonic decays using the full run II integrated luminosity of 10.4 fb^{-1} in $p\bar{p}$ collisions at a center of mass energy of 1.96 MeV at the Fermilab Tevatron Collider [10]. Further the CMS Collaboration is accomplished a search for the $X(5568)$ state by using pp collision data collected at $\sqrt{s} = 8$ TeV and corresponding to an integrated luminosity of 19.7 fb^{-1} . With about 50000 B_s^0 signal candidates, no significant structure in the $B_s^0\pi^\pm$ invariant mass spectrum is found around the mass reported by the DØ Collaboration [11]. Also, the LHCb Collaboration did not confirm the existence of the $X(5568)$ [12], which makes some theorists consider the difficulty of explaining the $X(5568)$ as a genuine resonance [13, 14, 15].

Although there exist different opinions on $X(5568)$, re-observation of it in experiment ignites theorists enthusiasm of surveying exotic tetraquark states. For instance in the framework of QCD sum rule, Albuquerque et. al. investigated the $X(5568)$ state using the molecular interpolating currents BK , $B_s\pi$, B^*K , $B_s^*\pi$ and tetraquark currents with quantum numbers $J^P = 0^+$ and 1^+ . Their numerical results did not support the $X(5568)$ as a pure molecule or a tetraquark state. However, they suggested it to be a mixture of BK molecule and scalar $[ds\bar{b}\bar{u}]$ tetraquark state with a mixing angle $\sin 2\Theta \simeq 0.15$ [16]. Also they conclude that XZ states are good candidates for 1^+ and 0^+ molecules or/and four-quark states while the predictions for 1^- and 0^- states are about 1.5 GeV above $Y_{b,c}$ thresholds. To date, the resonance $X(5568)$ has triggered lots of theoretical studies, most of which speculated it to be a typical diquark-antidiquark state while the molecular state assignment is not privileged.

The mass of $X(5568)$ is too far (nearly 200 MeV) below from the $\bar{B}K$ threshold (5774 MeV) to be interpreted as a hadronic molecule of $\bar{B}K$. Additionally, the interaction of $B_s^0\pi^\pm$ is very weak and unable to form a bounded structure. The LHCb Collaboration scanned the invariant mass of $B_s^0\pi^\pm$ and no significant signal for a $B_s^0\pi^\pm$ resonance is seen at any value of mass and width in the range considered [12]. Also the authors of Ref. [17] deduced a lower limit for the masses of a possible $[ds\bar{b}\bar{u}]$ tetraquark state: 6019 MeV. Completing Ref. [17], Ref. [18] presented an analysis based on general properties of QCD to analyze the $X(5568)$ state. Notably, it was shown that the mass of the $[ds\bar{b}\bar{u}]$ tetraquark state must be bigger than the

sum of the masses of the B_s meson and the light quark-antiquark resonance leading to an estimate of the lower limit of $M_{bsud} \simeq 5.9$ GeV. Moreover, in Ref. [19] and [20] mass of $X_{b,c}$ are calculated both in axial-vector and scalar pictures, respectively. The results obtained in this framework were found to be nicely consistent with the experiments. Also in Ref. [21] mass of the X_b ground state calculated in the diquark-antidiquark picture in Relativistic Quark Model (RQM) are higher than experimentally measured values as presented in Tables 2 and Table 4 and in the framework of Non-Relativistic Quark Model (NRQM) as well [22].

If the $X(5568)$ has a four-quark structure, its partner state within the same multiplet must also exist. We assume that this state bears the same quantum numbers as its counterpart, i.e. $J^P = 1^+$ or $J^{PC} = 0^{++}$. We also accept that it has the internal structure $X_c = [su][\bar{c}\bar{d}]$ in the diquark-antidiquark model. Our aim is to determine the parameters of the state X_c , i.e. to find its mass and pole residue. If this partner state is not detected, one should put a big question mark on the existence of the $X(5568)$ signal. According to Ref. [23] charmed partner of the $X(5568)$ have more strong decay channels than the bottom partners. Especially, the experimental search for it are strongly called for in the $D_s\pi$, $D_s^*\pi$, and isovector \overline{DK} channels. Due to explain its exotic decay modes, Liu et al. once recommended a tetraquark structure for the $D_{sJ}(2632)$ signal observed by the SELEX collaboration [24]. The mass of this particle is very close to the X_c meson. So this can be the same particle with X_c . Unfortunately, $D_{sJ}(2632)$ was not confirmed by subsequent experiments.

Analyzing the thermal version [25] of this ambiguous state $X(5568)$ using Shifman-Vainshtein-Zakharov Sum Rule (SVZSR) model [26] can give us a different point of views. Hence, in this article we tentatively assume that $X(5568)$ and its charmed partner are exotic states and will focus on the scenario of tetraquark state based on the SVZSR at finite temperature using the deconfinement temperature $T_c = 155$ MeV [27, 28, 29, 30]. Our motivation for extension our computation to the high temperatures is to interpret the heavy-ion collision experiments more precisely. Moreover investigations of particles at finite temperatures can give us information on understanding of the nonperturbative dynamics of QCD, deconfinement and chiral phase transition. We explore the variation of the mass and pole residue values in terms of increasing temperature.

The article is arranged as follows. Section 2 is devoted to the description of the SVZSR approach at $T \neq 0$. The mass and pole residue sum rule expressions for the exotic bottomonium and charmonium states are calculated by carrying out the operator product expansion (OPE) up to condensates of dimension-6. Then our numerical results for these quantities for the relevant mesons are reported in Section 3. Section 4 is reserved for our conclusions.

Finally the explicit forms of all spectral density expressions obtained in the calculations are given in the Appendix.

2. Thermal SVZ Sum Rule Formalism

In this section we try to find the correlation function from both the physical side (phenomenological side or hadronic side) and the QCD side (OPE side or theoretical side). As stated in the SVZSR, we can look at the quarks from both inside and also outside of the hadrons, these two situation which is assumed as corresponding to the same physical case can be calculated via two different windows. Then equalizing the results coming from both sides, the sum rules for the hadronic parameters are obtained.

Now assuming the $X(5568)$ state as a bound $[su][\bar{b}\bar{d}]$ tetraquark state and its charmed partner X_c state as a $[su][\bar{c}\bar{d}]$ tetraquark state, the mass and pole residue sum rules of $X(5568)$ and X_c resonances are obtained in hot medium. In this study, Thermal SVZSR (TSVZSR) method is used having applied to a wide range of hadronic observables from the light to the heavy quark sector prosperously.

TSVZSR proposed by Bochkarev and Shaposhnikov has been yielding a brand-new research area [25, 31, 32, 33, 34, 35, 36]. The TSVZSR start with the two-point correlation function for the scalar $\Pi(q, T)$ and axial-vector $\Pi_{\mu\nu}(q, T)$ assumption, respectively:

$$\Pi(q, T) = i \int d^4x e^{iq \cdot x} \langle \Psi | \mathcal{T} \{ \eta(x) \eta^\dagger(0) \} | \Psi \rangle, \quad (1)$$

$$\Pi_{\mu\nu}(q, T) = i \int d^4x e^{iq \cdot x} \langle \Psi | \mathcal{T} \{ \eta_\mu(x) \eta_\nu^\dagger(0) \} | \Psi \rangle, \quad (2)$$

where Ψ denotes the hot medium state, $\eta(x)$ and $\eta_\mu(x)$ are the interpolating currents of the considered particles and \mathcal{T} represents the time ordered product [26, 37, 38]. The thermal average of any operator \hat{O} in thermal equilibrium can be asserted by the following expression:

$$\langle \hat{O} \rangle = \frac{Tr(e^{-\beta \mathcal{H}} \hat{O})}{Tr(e^{-\beta \mathcal{H}})}, \quad (3)$$

where \mathcal{H} is the QCD Hamiltonian, and being the T is the temperature of the heat bath, $\beta = 1/T$ is inverse temperature.

Chosen currents $\eta(x)$ and $\eta_\mu(x)$ must contain all the information of the related meson, like quantum numbers, quark contents and so on. In the following, we will consider the tetraquark states with quark contents $[su][\bar{b}\bar{d}]$

and $[su][\bar{c}\bar{d}]$. In the diquark-antidiquark model currents for the scalar and axial-vector states can be expressed as [39, 19, 20]:

$$\begin{aligned}\eta(x) &= \epsilon_{ijk}\epsilon_{imn} \left[s_j(x) C \gamma_\mu u_k(x) \right] \left[\bar{Q}_m(x) \gamma_\mu C \bar{d}_n(x) \right], \\ \eta_\mu(x) &= s_j^T(x) C \gamma_5 u_k(x) \left[\bar{Q}_j(x) \gamma_\mu C \bar{d}_k^T(x) - \bar{Q}_k(x) \gamma_\mu C \bar{d}_j^T(x) \right],\end{aligned}\quad (4)$$

respectively, where $Q = b$ or c represent heavy quarks, C is the charge conjugation and i, j, k, m, n are color indexes.

2.1. Physical Side

First we focus on the evaluation of the physical side of the correlation function in order to determine the mass and pole residue sum rules of $X(5568)$ and its charmed partner (hereafter we will symbolize $X(5568)$ as X_b and the charmed partner as X_c). To derive mass and pole residue TSVZSR, we begin with the correlation function with regard to the hadronic degrees of freedom. Then we embed the complete set of intermediate physical states possessing the same quantum numbers as the interpolating current. Later, carrying out the integral over x in Eqs. (1) and (2), the following expressions are obtained for the scalar and axial-vector assumptions, respectively:

$$\begin{aligned}\Pi^{\text{Phys}}(q, T) &= \frac{\langle \Psi | \eta | X_{b(c)}(q) \rangle \langle X_{b(c)}(q) | \eta^\dagger | \Psi \rangle}{m_{X_{b(c)}}^2(T) - q^2} \\ &+ \text{higher states},\end{aligned}\quad (5)$$

$$\begin{aligned}\Pi_{\mu\nu}^{\text{Phys}}(q, T) &= \frac{\langle \Psi | \eta_\mu | X_{b(c)}(q) \rangle \langle X_{b(c)}(q) | \eta_\nu^\dagger | \Psi \rangle}{m_{X_{b(c)}}^2(T) - q^2} \\ &+ \text{higher states},\end{aligned}\quad (6)$$

here $m_{X_{b(c)}}(T)$ is the temperature-dependent mass of $X_{b(c)}$. Temperature dependent pole residues $f_{X_{b(c)}}(T)$ are defined with the following matrix elements:

$$\langle \Psi | \eta | X_{b(c)}(q) \rangle = f_{X_{b(c)}}(T) m_{X_{b(c)}}(T), \quad (7)$$

$$\langle \Psi | \eta_\mu | X_{b(c)}(q) \rangle = f_{X_{b(c)}}(T) m_{X_{b(c)}}(T) \varepsilon_\mu, \quad (8)$$

here ε_μ is the polarization vector of the $X_{b(c)}$ state satisfying the following relation:

$$\varepsilon_\mu \varepsilon_\nu^* = \frac{q_\mu q_\nu}{m_{X_{b(c)}}^2(T)} - g_{\mu\nu}. \quad (9)$$

Then the correlation function depending on $m_{X_{b(c)}}(T)$ and $f_{X_{b(c)}}(T)$ can be written in the below forms for the scalar case

$$\Pi^{\text{Phys}}(q, T) = \frac{m_{X_{b(c)}}^2(T) f_{X_{b(c)}}^2(T)}{m_{X_{b(c)}}^2(T) - q^2} + \dots \quad (10)$$

and the axial-vector case:

$$\Pi_{\mu\nu}^{\text{Phys}}(q, T) = \frac{m_{X_{b(c)}}^2(T) f_{X_{b(c)}}^2(T)}{m_{X_{b(c)}}^2(T) - q^2} \left(\frac{q_\mu q_\nu}{m_{X_{b(c)}}^2(T)} - g_{\mu\nu} \right) + \dots, \quad (11)$$

respectively. To obtain the TSVZSR we select a structure consisting of $g_{\mu\nu}$ for the axial one from the $\Pi_{\mu\nu}^{\text{Phys}}(q, T)$, then using the coefficients of this structure and applying the Borel transformation,

$$\hat{\mathcal{B}}_{(q^2)}[\Pi(q^2)] \equiv \lim_{n \rightarrow \infty} \frac{(-q^2)^n}{(n-1)!} \left(\frac{d^n}{dq^{2n}} \Pi(q^2) \right)_{q^2=n/M^2}, \quad (12)$$

which improves the convergence of the OPE series and also enhances the ground state contribution. So the physical side for the scalar and axial-vector cases are acquired as;

$$\hat{\mathcal{B}}_{(q^2)}[\Pi^{\text{Phys}}(q, T)] = m_{X_{b(c)}}^2(T) f_{X_{b(c)}}^2(T) e^{-m_{X_{b(c)}}^2(T)/M^2}. \quad (13)$$

2.2. QCD Side

In this part, our purpose is to find the correlation function belonging to the QCD side. $\Pi^{\text{QCD}}(q, T)$ can be defined according to quark-gluon degrees of freedom. Similar to physical side, the correlation functions given in Eqs. (1) and (2) on the QCD side are expanded in terms of Lorentz structures as well

$$\begin{aligned} \Pi^{\text{QCD}}(q, T) &= \Gamma_0(q, T) \mathbf{I}, \\ \Pi_{\mu\nu}^{\text{QCD}}(q, T) &= \Gamma_1(q, T) g_{\mu\nu} + \text{other structures}, \end{aligned} \quad (14)$$

where $\Gamma_{0,1}(q, T)$ are the scalar functions in the Lorentz structures that are selected in this work. In the rest frame of the particle, related correlation functions are expressed with the dispersion integral,

$$\Pi^{\text{QCD}}(q, T) = \int_{\mathcal{M}^2}^{s_0(T)} \frac{\rho^{\text{QCD}}(s, T)}{(s - q^2)} ds + \dots, \quad (15)$$

where $\mathcal{M} = m_s + m_u + m_{b(c)} + m_d$ and the related spectral density can be expressed as

$$\rho^{QCD}(s, T) = \frac{1}{\pi} \text{Im}[\Pi^{QCD}(s, T)]. \quad (16)$$

After briefly giving the general definitions, now we can start to the computation for the OPE side placing the current expressions in Eq. (4) into the QCD correlation function in Eqs. (1) and (2) and then contracting the heavy and light quark fields, we have the following expressions for the scalar assumption:

$$\begin{aligned} \Pi^{QCD}(q, T) = & i\tilde{\epsilon}\epsilon \int d^4x e^{iq \cdot x} \left[\text{Tr}[\gamma_\nu \tilde{S}_s^{jj'}(x) \gamma_\mu S_u^{kk'}(x)] \right. \\ & \left. + \text{Tr}[\gamma_\mu \tilde{S}_d^{m'n}(-x) \gamma_\nu S_b^{m'm}(-x)] \right], \end{aligned} \quad (17)$$

and the axial-vector one:

$$\begin{aligned} \Pi_{\mu\nu}^{QCD}(q, T) = & i\tilde{\epsilon}\epsilon \int d^4x e^{iq \cdot x} \left[\text{Tr}[\gamma_5 \tilde{S}_s^{jj'}(x) \gamma_5 S_u^{kk'}(x)] \text{Tr}[\gamma_\mu \tilde{S}_d^{j'k}(-x) \gamma_\nu \tilde{S}_b^{k'j}(-x)] \right. \\ & - \text{Tr}[\gamma_5 \tilde{S}_s^{jj'}(x) \gamma_5 S_u^{kk'}(x)] \text{Tr}[\gamma_\mu \tilde{S}_d^{k'k}(-x) \gamma_\nu S_b^{j'j}(-x)] \\ & - \text{Tr}[\gamma_5 \tilde{S}_s^{jj'}(x) \gamma_5 S_u^{kk'}(x)] \text{Tr}[\gamma_\mu \tilde{S}_d^{j'j}(-x) \gamma_\nu S_b^{k'k}(-x)] \\ & \left. + \text{Tr}[\gamma_5 \tilde{S}_s^{jj'}(x) \gamma_5 S_u^{kk'}(x)] \text{Tr}[\gamma_\mu \tilde{S}_d^{k'k}(-x) \gamma_\nu S_b^{j'j}(-x)] \right], \end{aligned} \quad (18)$$

where the notation $\tilde{S}^{jj'}(x) = CS^{jj'T}(x)C$ is used for brevity. Also, we have used the shorthand notations $\epsilon = \epsilon_{ijk}\epsilon_{lmn}$ and $\tilde{\epsilon} = \epsilon_{i'j'k'}\epsilon_{i'm'n'}$ in Eqs. (17) and (18). The quark propagator in non-perturbative approach can be expressed with the quark and gluon condensates [37]. At finite temperature additional operators arise since the breakdown of Lorentz invariance by the choice of the thermal rest frame. The residual $O(3)$ invariance naturally brings in additional operators to the quark propagator in thermal case. The expected attitude of the thermal averages of these new operators is opposite to those of the Lorentz invariant old ones [40].

General form of the heavy-quark propagator in this calculation in the coordinate space can be expressed as in the below form:

$$\begin{aligned} S_Q^{ij}(x) = & i \int \frac{d^4k}{(2\pi)^4} e^{-ik \cdot x} \left[\frac{\delta_{ij}(\not{k} + m_Q)}{k^2 - m_Q^2} - \frac{gG_{ij}^{\alpha\beta} \sigma_{\alpha\beta}(\not{k} + m_Q) + (\not{k} + m_Q) \sigma_{\alpha\beta}}{4(k^2 - m_Q^2)^2} \right. \\ & \left. + \frac{g^2}{12} G_{\alpha\beta}^A G_A^{\alpha\beta} \delta_{ij} m_Q \frac{k^2 + m_Q \not{k}}{(k^2 - m_Q^2)^4} + \dots \right], \end{aligned} \quad (19)$$

where $G_A^{\alpha\beta}$ is the external gluon field, obeying $G_{ij}^{\alpha\beta} = G_A^{\alpha\beta} t_{ij}^A$ with A is color indices from 1 to 8, $t_{ij}^A = \lambda_{ij}^A/2$ and λ_{ij}^A are the Gell-Mann matrices. As for the thermal light-quark propagator S_q the following statement is employed:

$$\begin{aligned} S_q^{ij}(x) = & i \frac{\not{x}}{2\pi^2 x^4} \delta_{ij} - \frac{m_q}{4\pi^2 x^2} \delta_{ij} - \frac{\langle \bar{q}q \rangle_T}{12} \delta_{ij} - \frac{x^2}{192} m_0^2 \langle \bar{q}q \rangle_T \left[1 - i \frac{m_q}{6} \not{x} \right] \delta_{ij} \\ & + \frac{i}{3} \left[\not{x} \left(\frac{m_q}{16} \langle \bar{q}q \rangle_T - \frac{1}{12} \langle u^\mu \Theta_{\mu\nu}^f u^\nu \rangle \right) + \frac{1}{3} (u \cdot x) \not{u} \langle u^\mu \Theta_{\mu\nu}^f u^\nu \rangle \right] \delta_{ij} \\ & - \frac{i g_s G_{ij}^{\alpha\beta}}{32\pi^2 x^2} (\not{x} \sigma_{\mu\nu} + \sigma_{\mu\nu} \not{x}) - i \delta_{ij} \frac{x^2 \not{x} \langle \bar{q}q \rangle_T^2}{7776} g_s^2, \end{aligned} \quad (20)$$

where m_q implies the light quark mass, u_μ is the four-velocity of the heat bath, $\langle \bar{q}q \rangle_T$ is the temperature-dependent light quark condensate being the $q = u, d$ or s and $\Theta_{\mu\nu}^f$ is the fermionic part of the energy momentum tensor. Also, for the gluon condensate with regard to the gluonic part of the energy-momentum tensor $\Theta_{\lambda\sigma}^g$, the consecutive relation is employed (see for details Ref. [40]):

$$\begin{aligned} \langle Tr^c G_{\alpha\beta} G_{\mu\nu} \rangle = & \frac{1}{24} (g_{\alpha\mu} g_{\beta\nu} - g_{\alpha\nu} g_{\beta\mu}) \langle G_{\lambda\sigma}^a G^{a\lambda\sigma} \rangle \\ & + \frac{1}{6} \left[g_{\alpha\mu} g_{\beta\nu} - g_{\alpha\nu} g_{\beta\mu} - 2(u_\alpha u_\mu g_{\beta\nu} - u_\alpha u_\nu g_{\beta\mu} \right. \\ & \left. - u_\beta u_\mu g_{\alpha\nu} + u_\beta u_\nu g_{\alpha\mu}) \right] \langle u^\lambda \Theta_{\lambda\sigma}^g u^\sigma \rangle. \end{aligned} \quad (21)$$

The imaginary part of the spectral density can be extracted by applying the following equality for $n \geq 2$:

$$\Gamma\left(\frac{D}{2} - n\right) \left(-\frac{1}{L}\right)^{\frac{D}{2}-n} \rightarrow \frac{(-1)^{n-1}}{(n-2)!} (-L)^{n-2} \ln(-L) \quad (22)$$

and then replacing $D \rightarrow 4$ and also, we can adopt the principal value prescription:

$$\frac{1}{s - m_{X_{b(c)}}} = PV \frac{1}{s - m_{X_{b(c)}}} - i\pi \delta(s - m_{X_{b(c)}}). \quad (23)$$

Then we substitute the propagators into the correlation functions and related integrals are performed. To remove the contributions originating from higher states we enforce the standard Borel transformation in terms of q^2 in the invariant amplitude, selecting the structures $g_{\mu\nu}$ and unit matrix for the axial-vector and scalar states, respectively in both physical and QCD side, equalizing the attained statement with the related part of $\hat{\mathcal{B}}(q^2) \Pi^{\text{Phys}}(q, T)$,

finally the pole residue SVZSR for X_b and X_c particles are extracted at finite temperature:

$$m_X^2(T) f_X^2(T) e^{-m_X^2(T)/M^2} = \int_{\mathcal{M}^2}^{s_0(T)} ds \rho^{\text{QCD}}(s, T) e^{-s/M^2}. \quad (24)$$

In order to find the mass TSVZSR we should expel the hadronic pole residue somehow, i.e. taking the derivative of the pole residue sum rule in Eq. (24) in terms of $(-1/M^2)$ and next dividing by itself, we can reach the thermal mass SVZSR of the considered hadronic state being M^2 the Borel mass parameter and $s_0(T)$ thermal continuum threshold parameter, respectively:

$$m_X^2(T) = \frac{\int_{\mathcal{M}^2}^{s_0(T)} ds s \rho^{\text{QCD}}(s, T) e^{-s/M^2}}{\int_{\mathcal{M}^2}^{s_0(T)} ds \rho^{\text{QCD}}(s, T) e^{-s/M^2}}. \quad (25)$$

For compactness, the explicit forms of all spectral densities are presented in Appendix.

3. Numerical Analysis

In this section, we find out the numerical values of mass and pole residue of $X_{b(c)}$ states both at the QCD vacuum and also $T \neq 0$ case. By analyzing the calculations one can see the hot medium effects on the hadronic parameters of the investigated state. During the computations, we used the input parameters in Table 1.

Table 1. Input parameters [41, 26, 37, 42]

Parameters	Values
$m_u = (2.9 \pm 0.6) \text{ MeV}$	$\langle 0 \bar{q}q 0 \rangle = -(0.24 \pm 0.01)^3 \text{ GeV}^3$
$m_d = (5.2 \pm 0.9) \text{ MeV}$	$\langle 0 \frac{\alpha_s G^2}{4} 0 \rangle = (0.022 \pm 0.004) \text{ GeV}^4$
$m_s = (95 \pm 5) \text{ MeV}$	$\langle 0 \bar{s}s 0 \rangle / \langle 0 \bar{q}q 0 \rangle = 0.8$
$m_b = (4.18 \pm 0.03) \text{ GeV}$	$m_0^2 = (0.8 \pm 0.2) \text{ GeV}^2$
$m_c = (1.275 \pm 0.025) \text{ GeV}$	

In addition to these input parameters, we need the temperature-dependent quark and gluon condensates, and the energy density expressions, too. For the thermal quark condensate, the fit function attained in Ref. [43] by fitting Lattice data [44] is used, being the light quark vacuum condensate $\langle 0 | \bar{q}q | 0 \rangle$, thermal version of quark condensate is determined as:

$$\langle \bar{q}q \rangle_T = \langle 0 | \bar{q}q | 0 \rangle (A e^{\alpha T} + B)^{3/2}. \quad (26)$$

In Eq. (26) $\alpha = 0.0412 \text{ MeV}^{-1}$, $A = -6.444 \times 10^{-4}$, and $B = 0.994$ are coefficients of the fit function. For the temperature-dependent gluon condensate found from Lattice QCD data [45], the following parametrization is employed:

$$\langle G^2 \rangle = \langle 0|G^2|0 \rangle \left[C + D \left(e^{\beta T - \gamma} + 1 \right)^{-1} \right], \quad (27)$$

with the coefficients $\beta = 0.13277 \text{ MeV}^{-1}$, $\gamma = 19.3481$, $C = 0.55973$ and $D = 0.43827$, $\langle 0|G^2|0 \rangle$ is the gluon condensate in vacuum state and $G^2 = G_{\alpha\beta}^A G_A^{\alpha\beta}$. Additionally, the gluonic and fermionic parts of the energy density parametrization is included to the calculation achieved in Ref. [46] from the Lattice QCD graphics given in Ref. [47]:

$$\begin{aligned} \langle \Theta_{00}^g \rangle &= \langle \Theta_{00}^f \rangle = \frac{1}{2} \langle \Theta_{00} \rangle \\ &= T^4 e^{(\lambda_1 T^2 - \lambda_2 T)} + ET^5. \end{aligned} \quad (28)$$

where $\lambda_1 = 113.867 \text{ GeV}^{-2}$, $\lambda_2 = 12.190 \text{ GeV}^{-1}$ and $E = -10.141 \text{ GeV}^{-1}$. To continue the computation one should also determine the temperature-dependent continuum threshold for the $X_{b(c)}$ state which is an auxiliary parameters in the model. The continuum threshold expression is generated by [43];

$$\frac{s_0(T)}{s_0} = \left[\frac{\langle \bar{q}q \rangle_T}{\langle 0|\bar{q}q|0 \rangle} \right]^{2/3}, \quad (29)$$

where s_0 is the continuum threshold at zero temperature. Actually this parameter is not completely arbitrary but characterizes the beginning of the first excited state with the same quantum numbers as the chosen interpolating currents for the considered particle. The working region for the s_0 is determined so that the physical quantities show relatively weak dependence on it.

Next, we discuss the employed parameter region of continuum threshold s_0 and Borel mass parameter M^2 , which is mainly restricted by the convergence of the OPE. The idea of the SVZSR method dictate us that the physical quantities should be independent of the continuum threshold s_0 and Borel mass parameter M^2 . After some analyzes, we defined the range of Borel parameter M^2 and continuum threshold s_0 such that hadronic parameters are stable at these intervals. We looked for the OPE convergence and the pole contribution dominance and determined the conventional Borel window in the SVZSR approach to ensure the quality of the analysis. The lower bound of the Borel parameter M_{\min}^2 is fixed from convergence of the

OPE. By quantifying this constraint we require that contributions of the last terms, that is dimension five plus six, in OPE are found around 15%.

$$\frac{\Pi^{(\text{Dim5+Dim6})}(M_{\min}^2, s_0)}{\Pi(M_{\min}^2, s_0)} \cong 0.15. \quad (30)$$

We also get an upper limit constraint for M_{\max}^2 by imposing the severe constraint that the QCD continuum contribution must be smaller than the pole contribution:

$$\text{PC}(s_0, M^2) = \frac{\Pi(M_{\max}^2, s_0)}{\Pi(M_{\max}^2, \infty)} > \frac{1}{2}. \quad (31)$$

Finally, a working region for M^2 and s_0 are fixed according to the above mentioned criteria, thus we arrive the following interval for the X_b :

$$M^2 \in [4 - 6] \text{ GeV}^2 \quad ; \quad s_0 \in [34.8 - 36.8] \text{ GeV}^2,$$

and for the X_c state:

$$M^2 \in [2 - 4] \text{ GeV}^2 \quad ; \quad s_0 \in [8.6 - 9.8] \text{ GeV}^2.$$

In this region the dependence of the mass and pole residue on s_0 and M^2 is fixed anymore, and we guarantee that the sum rules give the reliable results. Plotting the mass versus M^2 at different fixed values of the continuum threshold s_0 in figure 1 at $T = 0$ we see the independence of mass from M^2 . Numerical results obtained for the mass and pole residue in vacuum are shown in Table 2-Table 5 and our results are consistent with the results existing in the literature [7, 39, 19, 20].

Table 2. Comparison of the mass and pole residue vacuum values of X_b for the “scalar case” with theoretical models and experimental results available in the literature.

Parameter	$m_{X_b}(\text{MeV})$	$f_{X_b}(\text{GeV}^4)$
Present Work	5567_{-114}^{+112}	$(0.35_{-0.06}^{+0.07}) \times 10^{-2}$
Experiment	5567.8 ± 2.9 [7]	—
RQM	5997 [21]	—
NRQM	5980 [22] or 5901	—
SVZSR	5580 ± 140 [39]	—
SVZSR	5584 ± 137 [19]	$(0.24 \pm 0.02) \times 10^{-2}$ [19]

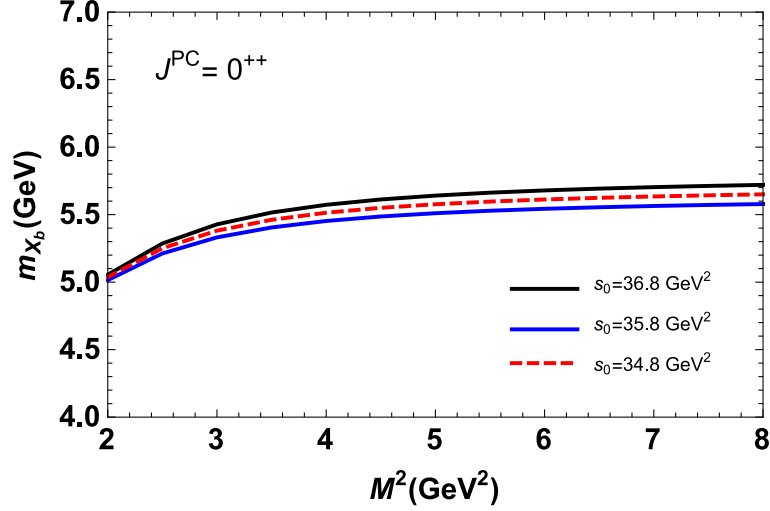


Fig. 1. The mass of X_b state versus the Borel mass parameter M^2 .

Table 3. Comparison of the mass and pole residue vacuum values of X_c for the “scalar case” with theoretical models and experimental results available in the literature.

Parameter	$m_{X_c}(\text{MeV})$	$f_{X_c}(\text{GeV}^4)$
Present Work	2675^{+128}_{-131}	$(0.39^{+0.07}_{-0.06}) \times 10^{-2}$
Experiment	—	—
RQM	2619 [21]	—
SVZSR	2550 ± 90 [39]	—
SVZSR	2634 ± 62 [20]	$(0.11 \pm 0.02) \times 10^{-2}$

Our last target is to look for the variations of the mass and pole residue of the X_b and X_c resonances in terms of temperature. Mass and pole residue versus temperature plots are drawn in figures 2-5.

This graphs display that the mass and pole residue of the X_b state stay roughly unmodified until $T \cong 0.12$ GeV, nonetheless, after this point, they begin to decrease promptly with increasing temperature. However diminishing of the mass and pole residue value with the temperature does not mean a stability of the studied state. To make a general deduction on the stability of the particle one should compute its decay width as well. Actually, similar to the mass and pole residue, the decay width of the particle depends also on the temperature. For instance in Ref. [48, 49] despite decreasing of the considered particles’ mass and pole residue in terms of temperature,

Table 4. Comparison of the mass and pole residue vacuum values of X_b for the “axial case” with theoretical models and experimental results available in the literature.

Parameter	$m_{X_b}(\text{MeV})$	$f_{X_b}(\text{GeV}^4)$
Present Work	5569^{+103}_{-102}	$(0.22^{+0.04}_{-0.03}) \times 10^{-2}$
Experiment	5567.8 ± 2.9 [7]	—
RQM	6125 [21] or 6021	—
SVZSR	5590 ± 150 [39]	—
SVZSR	5864 ± 158 [19]	$(0.42 \pm 0.14) \times 10^{-2}$ [19]

Table 5. Comparison of the mass and pole residue vacuum values of X_c for the “axial case” with theoretical models and experimental results available in the literature.

Parameter	$m_{X_c}(\text{MeV})$	$f_{X_c}(\text{GeV}^4)$
Present Work	2557^{+124}_{-122}	$(6.08^{+0.78}_{-0.74}) \times 10^{-2}$
Experiment	—	—
SVZSR	2550 ± 100 [39]	—

decay widths are increased with the temperature.

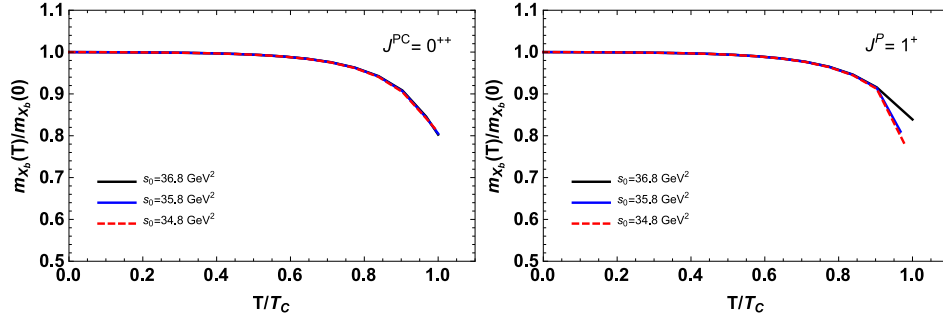


Fig. 2. Mass changes as a function of temperature of scalar (Left) and axial-vector X_b state (Right).

4. Conclusion

In this work, we have revisited the bottomonium and charmonium states X_b and X_c extending our model from vacuum state to heat bath. To describe

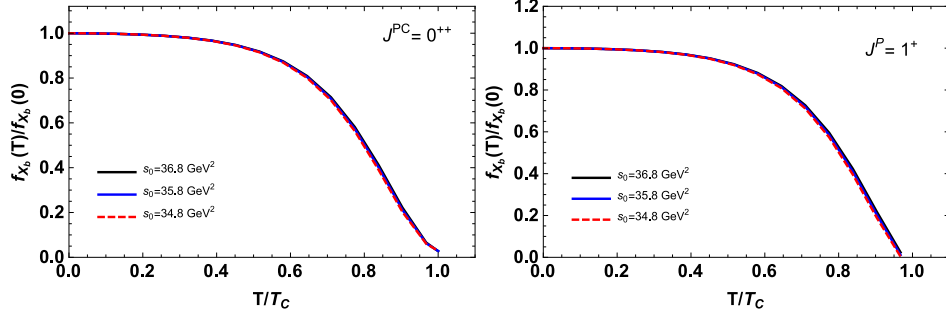


Fig. 3. Pole residue variations as a function of temperature of scalar (Left) and axial-vector X_b state (Right).

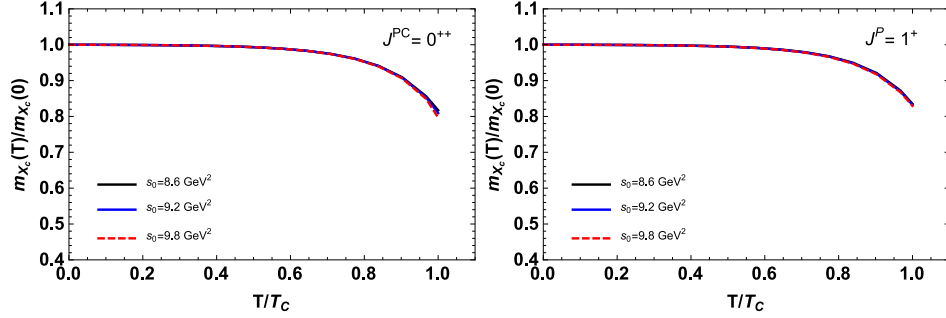


Fig. 4. Mass changes in terms of temperature of scalar (Left) and axial-vector X_c state (Right).

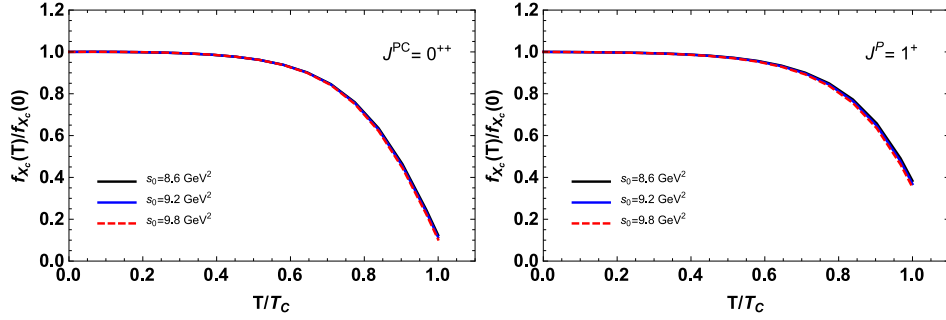


Fig. 5. Pole residue variations in terms of temperature of scalar (Left) and axial-vector X_c state (Right).

the effects of hot medium to the hadronic parameters of the resonances X_b and X_c , Thermal SVZSR model is used considering contributions of condensates up to dimension six. We hope that renew interpretation of X_b resonance in hot medium may give different insights for understanding the inner structure of unfitted bottomonium states with Quark Model. Due to its observed decay mode, the X_b must contain four different valence quark components, which makes the X_b a good candidate for a tetraquark state.

We investigate this state in axial-vector and scalar picture as tetraquark candidate. Numerical findings show that the X_b can be well described by both scalar and axial-vector tetraquark currents. This particle has almost equal possibility for being a scalar or axial-vector particle. Our results at $T = 0$ are in reasonable agreement with the available experimental data and other SVZSR works in the literature. The exact result can only be determined by the precise measurement of the decay width values by the experiments. Additionally, our numerical calculations indicate that the mass and pole residue values of the considered states are stable at low temperatures, but they reduce by roughly 20% and 98% of their vacuum values for the X_b state and also for the charmed partner 20% and 90%, respectively when the temperature approaches to phase transition temperature for the scalar assumption. In the axial-vector picture, these values decrease by 17% and 99% of their vacuum values for the X_b , 18% and 65% of its charmed partner, too.

There are some comments on that this decrease can indicate the deconfinement phase transition in quark-gluon plasma which also occur in the early universe. In the literature, remarkable drop in the values of mass and pole residue in hot medium can be regarded as the signal of the quark-gluon plasma (QGP), called as new state of matter, phase transition. Also, the manner of X_b state according to temperature can be a useful tool to analyze the heavy-ion collision experiments. Our estimates for the hadronic features of the X_b meson can be tested in the forthcoming experiments such as CMS, LHCb and PANDA.

The X_b data will provide a rich physics output and this makes a motivated issue for the Belle-II initial data taking. We hope that precise spectroscopic measurements are predicted at the Super-B factories and at the LHC will supply conclusive answers to open questions raised here such as unconventional quark combinations, interactions in exotic hadrons, etc. and will help resolve the current and long-standing puzzles in the exotic bottomonium and charmonium sectors.

However, the production mechanism of the X_b is very different at the $p\bar{p}$ and pp colliders. Future experimental efforts are desirable in the clarification of the situation on the X_b state and its charmed partner. In 2004 SELEX Collaboration [24] reported the first observation of a charm-strange meson

$D_{sJ}^+(2632)$ at a mass of 2632.5 ± 1.7 MeV/c², the charm hadro-production experiment E781 at Fermilab. Since this particle has nearly the same mass as the X_c that was discovered in the SELEX experiment, it may most likely be the same particle.

Further detailed experimental and theoretical studies of the invariant mass of $B_s^0 \pi^\pm$ spectrum, production and decays of tetraquark states with four different flavors in the future are severely called for towards a better understanding their nature and the classification of exotics.

Appendix A

The spectral densities

In this appendix the results of the spectral densities in our calculations are presented. The spectral density can be written separating the terms according to the operator dimensions as:

$$\rho^{\text{QCD}}(s, T) = \rho^{\text{pert.}}(s) + \rho^{\text{non-pert.}}(s, T). \quad (\text{A.1})$$

Here,

$$\begin{aligned} \rho^{\text{non-pert.}}(s, T) &= \rho^{\langle \bar{q}q \rangle}(s, T) + \rho^{\langle G^2 \rangle + \langle \Theta_{00} \rangle}(s, T) \\ &+ \rho^{\langle \bar{q}Gq \rangle}(s, T) + \rho^{\langle \bar{q}q \rangle^2}(s, T). \end{aligned} \quad (\text{A.2})$$

The complete expressions for $\rho^{\text{pert.}}(s)$ and $\rho^{\text{nonpert.}}(s, T)$ are shown below as the integrals over the Feynman parameter z for the axial assumption ($J^P = 1^+$) of $X(5568)$:

$$\begin{aligned} \rho^{\text{pert.}}(s) &= \frac{1}{3 \times 2^{12} \pi^6} \int_0^1 dz \frac{1}{r^3} \left\{ z^2 (rs + m_b^2)^2 \left[z \left(5s^2 z \zeta + 6\phi s m_b^2 + z m_b^4 \right. \right. \right. \\ &\quad \left. \left. - 16m_b m_d (rs + m_b^2) \right) + 16m_s m_u \left(4sz \zeta + \phi m_b^2 - 9rm_b m_d \right) \right] \right\} \\ &\times \theta[L(s, z)], \end{aligned} \quad (\text{A.3})$$

$$\begin{aligned} \rho^{\langle \bar{q}q \rangle}(s, T) &= \frac{1}{2^7 \pi^4} \int_0^1 dz \frac{1}{r^2} \left\{ z \left[r(rs + m_b^2) (3\phi s + z m_b^2 - 4m_b m_d) \right. \right. \\ &\times \left\{ m_s (\langle s\bar{s} \rangle - 2\langle u\bar{u} \rangle) + m_u (-2\langle s\bar{s} \rangle + \langle u\bar{u} \rangle) \right\} + \langle d\bar{d} \rangle \left[2z m_b^5 + \phi m_b^4 m_d \right. \\ &\quad \left. + 4\zeta m_b^2 m_d (sz + m_s m_u) + 4rm_b^3 (sz + 2m_s m_u) + 2s\zeta m_b (sz + 4m_s m_u) \right. \\ &\quad \left. \left. \left. + s\phi m_d (3sz + 8m_s m_u) \right] \right] \right\} \theta[L(s, z)], \end{aligned} \quad (\text{A.4})$$

$$\begin{aligned}
 \rho^{\langle G^2 \rangle + \langle \Theta_{00} \rangle}(s, T) = & \frac{1}{\pi^4} \left\langle \frac{\alpha_s G^2}{\pi} \right\rangle \int_0^1 dz \frac{1}{9 \times 2^5} \left\{ \frac{1}{r^3} z \left[4s^2 \varphi z (-27 + 32z) \right. \right. \\
 & + m_b \left\{ 2\phi s m_b \left(72 + z(-160 + 89z) \right) + (6 - 7z)^2 m_b^3 - 4\zeta m_d \left[s(-36 \right. \right. \\
 & + z(36 + z)) + 36m_b^2 \left. \right] \left. \right\} + 4\phi m_s m_u \left(24s\varphi + (-18 + 19z)m_b^2 \right) \left. \right] \theta[L(s, z)] \\
 & + \frac{\langle \Theta_{00}^f \rangle}{32r} \left[z \left(s^2 z 3 + 80z \right) \zeta + m_b \left\{ 72\phi s z m_b + z(-3 + 8z)m_b^3 - 24r m_d \right. \right. \\
 & \left. \left(s(-1 + 3z) + m_b^2 \right) \right\} + 12r m_s m_u (4rs + m_b^2) \left. \right] \\
 & + \frac{\langle \Theta_{00}^g \rangle}{8\pi^2 r^2} g_s^2 z \zeta \left[s^2 z (-1 + 4z)(-9 + 10z) + m_b \left\{ 4\phi s m_b \left(3 + z(-11 + 9z) \right) \right. \right. \\
 & + z(3 - 6z + 4z^2)m_b^3 - 12\zeta \left[s m_d \left((-1 + 3z) + m_b^2 \right) \right] \left. \right\} \\
 & \left. + 6\phi m_s m_u (2rs + m_b^2) \right] \left. \right\}, \tag{A.5}
 \end{aligned}$$

$$\begin{aligned}
 \rho^{\langle \bar{q} G q \rangle}(s, T) = & \frac{1}{3 \times 2^6 \pi^4} \int_0^1 dz \frac{m_0^2}{r} \left\{ r \left(2\phi s + z m_b^2 - m_b m_d \right) \left[m_s (\langle s \bar{s} \rangle - 3 \right. \right. \\
 & \times \langle u \bar{u} \rangle) + m_u (-3 \langle s \bar{s} \rangle + \langle u \bar{u} \rangle) \left. \right] + \langle d \bar{d} \rangle \left[3z m_b^3 + \phi m_b^2 m_d + 3r m_b (sz + m_s \right. \\
 & \times m_u) + \zeta m_d (2sz + m_s m_u) \left. \right] \left. \right\} \tag{A.6}
 \end{aligned}$$

and

$$\begin{aligned} \rho^{\langle \bar{q}q \rangle^2}(s, T) = & \frac{1}{3 \times 2^4 \pi^2} \int_0^1 dz \left\{ \frac{1}{27 \pi^2} \left[g_s^2 \left(\langle s\bar{s} \rangle^2 + \langle u\bar{u} \rangle^2 \right) (2\phi s + z m_b^2 \right. \right. \\ & - m_b m_d) + 27 \langle d\bar{d} \rangle \pi^2 (2m_b + r m_d) \left[m_s (\langle s\bar{s} \rangle - 2\langle u\bar{u} \rangle) + m_u (-2\langle s\bar{s} \rangle \right. \\ & + \langle u\bar{u} \rangle) \left. \right] + \langle d\bar{d} \rangle^2 g_s^2 (2rsz + z m_b^2 + r m_s m_u) + 27 \pi^2 \langle s\bar{s} \rangle \langle u\bar{u} \rangle (8rsz + 4z \\ & \left. \left. \times m_b^2 - 4m_b m_d + r m_s m_u) \right] \right\} \theta[L(s, z)] + \langle s\bar{s} \rangle \langle u\bar{u} \rangle m_b m_d m_s m_u \delta(s - m_b^2). \end{aligned} \quad (\text{A.7})$$

For the scalar assumption ($J^{PC} = 0^{++}$) we get the following expressions for the spectral density as follows:

$$\begin{aligned} \rho^{\text{pert.}}(s) = & \frac{1}{3 \times 2^9 \pi^6} \int_0^1 dz \frac{1}{r^3} \left\{ \left[z^2 (rs + m_b^2)^2 \left\{ -z \left(3s^2 z \zeta + 4\phi s m_b^2 + z m_b^4 \right) + \right. \right. \right. \\ & \left. \left. 4z m_b m_d (rs + m_b^2) - 4m_s m_u \left(5sz \zeta + 2m_b (\phi m_b - 9rm_d) \right) \right\} \right] \right\} \theta[L(s, z)], \quad (\text{A.8}) \end{aligned}$$

$$\begin{aligned} \rho^{\langle q\bar{q} \rangle}(s, T) = & -\frac{1}{2^5 \pi^4} \int_0^1 dz \frac{1}{r^2} \left\{ z \left[2r(rs + m_b^2) \left\{ 2\phi s \left(\langle s\bar{s} \rangle - \langle u\bar{u} \rangle \right) (m_s - m_u) \right. \right. \right. \\ & + \left(\langle s\bar{s} \rangle - \langle u\bar{u} \rangle \right) z m_b^2 (m_s - m_u) - m_b m_d \left(m_s (\langle s\bar{s} \rangle - 4\langle u\bar{u} \rangle) + m_u (-4\langle s\bar{s} \rangle \right. \\ & + \langle u\bar{u} \rangle) \left. \right) \left. \right\} + \langle d\bar{d} \rangle \left[z m_b^5 + 2\phi m_b^4 m_d + 2\zeta m_b^2 m_d (3sz + 2m_s m_u) + 2s\varphi m_d (2sz \right. \\ & \left. + 3m_s m_u) + 2r m_b^3 (sz + 4m_s m_u) + s m_b \zeta (sz + 8m_s m_u) \right] \left. \right] \right\} \theta[L(s, z)], \quad (\text{A.9}) \end{aligned}$$

$$\begin{aligned}
 \rho^{\langle G^2 \rangle + \langle \Theta_{00} \rangle}(s, T) = & \frac{1}{6^2 \pi^4} \langle \frac{\alpha_s G^2}{\pi} \rangle \int_0^1 dz \frac{1}{64} \left\{ \frac{1}{r^3} \left[-2zm_b^4 \left(18 + z(-30 + 13z) \right) \right. \right. \\
 & + 2\zeta sm_b m_d \left(36 + (-54 + z)z \right) + 36m_b^3 m_d r(2 - 3z) - 12s\varphi z(-6s + 4sz \\
 & + 9m_s m_u) + \phi m_b^2 \left(-3s(6 - 5z)^2 + 4m_s m_u(18 - 19z) \right) \left. \right] + \frac{\langle \Theta_{00}^f \rangle}{r^2} \left[z \left(r s^2 \right. \right. \\
 & \times (3 - 50z)z\zeta + 3m_b \left\{ \phi r s m_b(3 - 16z) - 2z\zeta m_b^3 + 2m_d \left(r^2 s(-1 + 3z) + \zeta m_b^2 \right) \right\} \\
 & \left. \left. - 9\zeta r s m_s m_u \right) \right] - \frac{\langle \Theta_{00}^g \rangle}{14\pi^2 r^2} \left[g_s^2 z \left(\phi s m_b^2 \left(3 + 4z(-3 + 2z) \right) + 3z\zeta m_b^4 + 3r s m_b m_d \right. \right. \\
 & \times \left(2 + z(-9 + 8z) \right) + m_b^3 m_d \left(6 + z(-15 + 8z) \right) + s z \zeta \left\{ s[6 + z(-34 \right. \\
 & \left. \left. + 25z) + 9m_s m_u \right\} \right) \left. \right] \left. \right\} \theta[L(s, z)] - \frac{1}{r} \langle \frac{\alpha_s G^2}{\pi} \rangle m_b m_d m_s m_u s z^2 \delta\left(s + \frac{m_b^2}{r}\right), \quad (\text{A.10})
 \end{aligned}$$

$$\begin{aligned}
 \rho^{\langle \bar{q} G q \rangle}(s, T) = & \frac{1}{3 \times 2^5 \pi^4} \int_0^1 dz \frac{m_0^2}{r} \left\{ 3\langle d\bar{d} \rangle z m_b^3 + 3\phi r s \left[m_s \left(2\langle s\bar{s} \rangle - 3\langle u\bar{u} \rangle \right) + m_u \right. \right. \\
 & \times \left(-3\langle s\bar{s} \rangle + 2\langle u\bar{u} \rangle \right) \left. \right] + 2\langle d\bar{d} \rangle \zeta m_d (3sz + m_s m_u) + m_b^2 \left[4\langle d\bar{d} \rangle \phi m_d + 2rz \left\{ m_s \right. \right. \\
 & \times (2\langle s\bar{s} \rangle - 3\langle u\bar{u} \rangle) + m_u (-3\langle s\bar{s} \rangle + 2\langle u\bar{u} \rangle) \left. \right\} \left. \right] + r m_b \left[-m_d \left\{ m_s \left(\langle s\bar{s} \rangle - 6\langle u\bar{u} \rangle \right) \right. \right. \\
 & \left. \left. + m_u (-6\langle s\bar{s} \rangle + \langle u\bar{u} \rangle) \right\} + 3\langle d\bar{d} \rangle \left(sz + 2m_s m_u \right) \right] \left. \right\} \theta[L(s, z)], \quad (\text{A.11})
 \end{aligned}$$

and

$$\begin{aligned}
 \rho^{\langle \bar{q} q \rangle^2}(s, T) = & -\frac{1}{3 \times 2^3 \pi^2} \int_0^1 dz \frac{1}{27\pi^2} \left\{ g_s^2 \left(\langle s\bar{s} \rangle^2 + \langle u\bar{u} \rangle^2 \right) (6\phi s + 4zm_b^2 - m_b m_d) \right. \\
 & + 2\langle d\bar{d} \rangle^2 g_s^2 \left(3rsz + 2zm_b^2 + rm_s m_u \right) + 108\pi^2 \langle s\bar{s} \rangle \langle u\bar{u} \rangle (3rsz + 2zm_b^2 - 2m_b m_d \\
 & + rm_s m_u) + 54\langle d\bar{d} \rangle \pi^2 \left[2rm_d(m_s - m_u) \left(\langle s\bar{s} \rangle - \langle u\bar{u} \rangle \right) + m_b \left\{ m_s \left(\langle s\bar{s} \rangle - 4\langle u\bar{u} \rangle \right) \right. \right. \\
 & \left. \left. + m_u \left(-4\langle s\bar{s} \rangle + \langle u\bar{u} \rangle \right) \right\} \right] \left. \right\} \theta[L(s, z)] - \langle s\bar{s} \rangle \langle u\bar{u} \rangle m_b m_d m_s m_u \delta(s - m_b^2) \quad (\text{A.12})
 \end{aligned}$$

where the explicit expression of the function $L(s, z)$ is

$$L(s, z) = sz(1 - z) - zm_b^2. \quad (\text{A.13})$$

In the expressions above the following abbreviations is used for simplicity:

$$\begin{aligned} \varphi &= (z - 1)^3, \\ \zeta &= (z - 1)^2, \\ \phi &= z(z - 1), \\ r &= z - 1. \end{aligned} \quad (\text{A.14})$$

If one makes the replacement $m_b \rightarrow m_c$, the spectral density of the charmed partner of $X(5568)$ can be easily obtained.

REFERENCES

- [1] S. K. Choi *et al.* [Belle Collaboration], *Phys. Rev. Lett.*, **91**, 262001 (2003).
- [2] S. Godfrey and S. L. Olsen, *Ann. Rev. Nucl. Part. Sci.*, **58**, 51 (2008).
- [3] A. Esposito, A. L. Guerrieri, F. Piccinini, A. Pilloni and A. D. Polosa, *Int. J. Mod. Phys. A*, **30**, 1530002 (2015).
- [4] X. Liu, *Chin. Sci. Bull.*, **59**, 3815 (2014).
- [5] S. L. Olsen, *Front. Phys.* (Beijing), **10**, 121 (2015).
- [6] R. L. Jaffe, *Phys. Rev. D*, **15**, 267 (1977).
- [7] V. M. Abazov *et al.* [D0 Collaboration], *Phys. Rev. Lett.*, **117**, 022003 (2016).
- [8] T. Aaltonen *et al.* [CDF Collaboration], *Phys. Rev. Lett.*, **120**, 202006 (2018).
- [9] M. Aaboud *et al.* [ATLAS Collaboration], *Phys. Rev. Lett.*, **120**, 202007 (2018).
- [10] V. M. Abazov *et al.* [D0 Collaboration], *Phys. Rev. D*, **97**, 092004 (2018).
- [11] A. M. Sirunyan *et al.* [CMS Collaboration], *Phys. Rev. Lett.*, **120**, 202005 (2018).
- [12] R. Aaij *et al.* [LHCb Collaboration], *Phys. Rev. Lett.*, **117**, 152003 (2016) Addendum: [*Phys. Rev. Lett.*, **118**, 109904 (2017)].
- [13] Z. Yang, Q. Wang and U. G. Meißner, *Phys. Lett. B*, **767**, 470 (2017).
- [14] R. M. Albuquerque, S. Narison, F. Fanomezana, A. Rabemananjara, D. Rabetiarivony and G. Randriamanatrika, *Nucl. Part. Phys. Proc.*, **83**, 282 (2017).
- [15] C. B. Lang, D. Mohler and S. Prelovsek, *Phys. Rev. D*, **94**, 074509 (2016).
- [16] R. Albuquerque, S. Narison, A. Rabemananjara and D. Rabetiarivony, *Int. J. Mod. Phys. A*, **31**, 1650093 (2016).
- [17] T. J. Burns and E. S. Swanson, *Phys. Lett. B*, **760**, 627 (2016).
- [18] F. K. Guo, U. G. Meißner and B. S. Zou, *Commun. Theor. Phys.*, **65**, 593 (2016).

- [19] S. S. Agaev, K. Azizi and H. Sundu, *Phys. Rev. D*, **93**, 074024 (2016).
- [20] S. S. Agaev, K. Azizi and H. Sundu, *Phys. Rev. D*, **93**, 094006 (2016).
- [21] D. Ebert, R. N. Faustov and V. O. Galkin, *Phys. Lett. B*, **696**, 241 (2011).
- [22] Z. Ghaleenovi, F. Giacosa and D. H. Rischke, *Acta Phys. Polon. B*, **47**, 1185 (2016).
- [23] Y. R. Liu, X. Liu and S. L. Zhu, *Phys. Rev. D*, **93**, 074023 (2016).
- [24] P. S. Cooper [SELEX Collaboration], eConf C, **0406271**, MONT01 (2004) [*Nucl. Phys. Proc. Suppl.*, **142**, 467 (2005)].
- [25] A. I. Bochkarev and M. E. Shaposhnikov, *Nucl. Phys. B*, **268**, 220 (1986).
- [26] M. A. Shifman, A. I. Vainshtein and V. I. Zakharov, *Nucl. Phys. B*, **147**, 385 (1979).
- [27] Y. Aoki, Z. Fodor, S. D. Katz and K. K. Szabo, *Phys. Lett. B* **643**, 46 (2006).
- [28] A. Andronic, P. Braun-Munzinger, K. Redlich and J. Stachel, *Nature* **561**, no. 7723, 321 (2018).
- [29] Steinbrecher, P. [HotQCD Collaboration], *Nucl. Phys. A* **982**, 847 (2019).
- [30] Bazavov A. *et al.*, *Phys. Rev. D* **95**, 5, 054504 (2017).
- [31] T. Hatsuda, Y. Koike and S. H. Lee, *Nucl. Phys. B*, **394**, 221 (1993).
- [32] J. Alam, S. Sarkar, P. Roy, T. Hatsuda and B. Sinha, *Annals Phys.*, **286**, 159 (2001).
- [33] R. Rapp, J. Wambach and H. van Hees, *Landolt-Bornstein*, **23**, 134 (2010).
- [34] S. Mallik and K. Mukherjee, *Phys. Rev. D*, **58**, 096011 (1998).
- [35] C. A. Dominguez, M. Loewe and Y. Zhang, *Phys. Rev. D*, **88**, 054015 (2013).
- [36] E. Veli Veliev, S. Günaydin and H. Sundu, *Eur. Phys. J. Plus*, **133**, 139 (2018).
- [37] L. J. Reinders, H. Rubinstein and S. Yazaki, *Phys. Rept.*, **127**, 1 (1985).
- [38] P. Colangelo and A. Khodjamirian, In Shifman, M. (ed.): At the frontier of particle physics, vol. **3**, 1495-1576 (2000).
- [39] W. Chen, H. X. Chen, X. Liu, T. G. Steele and S. L. Zhu, *Phys. Rev. Lett.*, **117**, 022002 (2016).
- [40] S. Mallik, *Phys. Lett. B*, **416** 373 (1998).
- [41] M. Tanabashi *et al.* [Particle Data Group], *Phys. Rev. D*, **98**, 030001 (2018) and (2019) update.
- [42] S. Narison, *Phys. Lett. B*, **693**, 559 (2010) Erratum: [*Phys. Lett. B*, **705**, 544 (2011)].
- [43] C. A. Dominguez and L. A. Hernandez, *Mod. Phys. Lett. A* **31**, no. 36, 1630042 (2016).
- [44] G. S. Bali, F. Bruckmann, G. Endrodi, Z. Fodor, S. D. Katz and A. Schafer, *Phys. Rev. D* **86**, 071502 (2012).
- [45] D. E. Miller, *Phys. Rept.* **443**, 55 (2007).
- [46] K. Azizi and G. Bozkır, *Eur. Phys. J. C* **76**, no. 10, 521 (2016).

- [47] M. Cheng *et al.*, *Phys. Rev. D*, **77**, 014511 (2008).
- [48] C. A. Dominguez, M. Loewe, J. C. Rojas and Y. Zhang, *Phys. Rev. D*, **81**, 014007 (2010).
- [49] K. Azizi and N. Er, *Phys. Rev. D*, **81**, 096001 (2010).